Reactive Oxygen Species and Nitric Oxide Mediate Actin Reorganization and Programmed Cell Death in the Self-Incompatibility Response of *Papaver*[1][W][OA]

Katie A. Wilkins[2], James Bancroft[2,3], Maurice Bosch[2,4], Jennifer Ings, Nicholas Smirnoff, and Vernonica E. Franklin-Tong*

School of Biosciences, College of Life and Environmental and Life Sciences, University of Birmingham, Edgbaston, Birmingham B15 2TT, United Kingdom (K.A.W., J.B., M.B., J.I., V.E.F.-T.); and Biosciences, College of Life and Environmental Sciences, University of Exeter, Exeter EX4 4QD, United Kingdom (N.S.)

Pollen-pistil interactions are critical early events regulating pollination and fertilization. Self-incompatibility (SI) is an important mechanism to prevent self-fertilization and inbreeding in higher plants. Although data implicate the involvement of reactive oxygen species (ROS) and nitric oxide (NO) in pollen-pistil interactions and the regulation of pollen tube growth, there has been a lack of studies investigating ROS and NO signaling in pollen tubes in response to defined, physiologically relevant stimuli. We have used live-cell imaging to visualize ROS and NO in growing *Papaver rhoeas* pollen tubes using chloromethyl-2′7′-dichlorodihydrofluorescein diacetate acetyl ester and 4-amino-5-methylamino-2′,7′-difluorofluorescein diacetate and demonstrate that SI induces relatively rapid and transient increases in ROS and NO, with each showing a distinctive "signature" within incompatible pollen tubes. Investigating how these signals integrate with the SI responses, we show that Ca^{2+} increases are upstream of ROS and NO. As ROS/NO scavengers alleviated both the formation of SI-induced actin punctate foci and also the activation of a DEVDase/caspase-3-like activity, this demonstrates that ROS and NO act upstream of these key SI markers and suggests that they signal to these SI events. These data represent, to our knowledge, the first steps in understanding ROS/NO signaling triggered by this receptor-ligand interaction in pollen tubes.

Pollen-pistil interactions in flowering plants are involved in pivotal events regulating pollination and fertilization. An important mechanism that operates during pollination to prevent inbreeding and its consequential debilitating effects is self-incompatibility (SI). Three distinct SI systems have been identified to date at the molecular level, which suggests that SI has evolved independently several times (for recent reviews, see Takayama and Isogai, 2005; Franklin-Tong, 2008). These systems use a variety of mechanisms to prevent self-fertilization. Despite being controlled by different genes, all the SI systems use an *S*-locus. Self-fertilization is prevented by use of a specific recognition system, which results in "self" pollen (i.e. incompatible pollen) being rejected at some point in the pollination process, while compatible pollen is allowed to grow freely. The *S*-locus is multiallelic, which allows for different specificities to be generated, and combinations of different haplotypes allow discrimination between self and nonself. When pollen *S*- and pistil *S*-haplotypes match, this creates an incompatible combination and incompatible pollen is rejected.

SI in *Papaver rhoeas* (the field poppy) has been studied particularly with respect to signaling in relation to the SI response triggered in incompatible pollen tubes. The *S*-locus comprises pollen and pistil *S*-determinants. The pistil *S*-determinant is a small approximately 15-kD protein, PrsS (previously called "S protein"), encoded by the pistil part of the *S*-locus (Foote et al., 1994). The pollen *S*-determinant, PrpS, is a small approximately 20-kD transmembrane protein (Wheeler et al., 2009). Interaction of PrsS with PrpS in an incompatible combination results in rapid inhibition of tip growth.

An incompatible interaction triggers almost instantaneous, large increases in cytosolic free Ca^{2+} ($[Ca^{2+}]_{cyt}$), which are visualized as a "wave" in the pollen tube "shank"; apical $[Ca^{2+}]_{cyt}$ is lost within a few minutes (Franklin-Tong et al., 1993, 1997). SI also stimulates Ca^{2+} and K^+ channel activity (Wu et al., 2011). The current working model proposes that PrsS proteins act as signaling ligands by interacting in an *S*-specific

[1] This work was supported by the Biotechnology and Biological Sciences Research Council (Ph.D. studentship to K.A.W.) and by the Wellcome Trust (summer studentship to J.B.).

[2] These authors contributed equally to the article.

[3] Present address: Centre for Mechanochemical Cell Biology, Warwick Medical School, University of Warwick, Coventry CV4 7AL, United Kingdom.

[4] Present address: Institute of Biological, Environmental, and Rural Sciences, Aberystwyth University, Plas Gogerddan, Aberystwyth SY23 3EB, United Kingdom.

* Corresponding author; e-mail v.e.franklin-tong@bham.ac.uk.

The author responsible for distribution of materials integral to the findings presented in this article in accordance with the policy described in the Instructions for Authors (www.plantphysiol.org) is: Vernonica E. Franklin-Tong (v.e.franklin-tong@bham.ac.uk).

[W] The online version of this article contains Web-only data.

[OA] Open Access articles can be viewed online without a subscription.

www.plantphysiol.org/cgi/doi/10.1104/pp.110.167510

manner with the pollen *S*-determinant. These initial interactions trigger a Ca^{2+}-dependent network, which culminates in programmed cell death (PCD), mediated by a DEVDase/caspase-3-like activity, resulting in the destruction of "self" pollen (Thomas and Franklin-Tong, 2004; Bosch and Franklin-Tong, 2007). Upstream of PCD, a number of SI-specific events are rapidly triggered in incompatible pollen. The F-actin and microtubule cytoskeleton are rapidly depolymerized, and the actin cytoskeleton further reorganizes to form stable "punctate foci" (Geitmann et al., 2000; Snowman et al., 2002; Poulter et al., 2008, 2010, 2011). Soluble inorganic pyrophosphatases, Pr-p26.1a and Pr-p26.1b, are phosphorylated and their activity inhibited (de Graaf et al., 2006). Both actin alterations (Thomas et al., 2006) and a mitogen-activated protein kinase (MAPK; p56; Li et al., 2007) play a role in the initiation of PCD. Thus, a relatively complex signaling network regulating SI in this species is emerging.

Both reactive oxygen species (ROS) and nitric oxide (NO) are well established as signaling molecules, mediating a wide range of cellular responses. There are numerous examples of ROS being involved in modulating biological responses, including hormone signaling involving growth and development, cell cycle, stress, defense responses, and PCD (Apel and Hirt, 2004; Laloi et al., 2004; Mittler et al., 2004; Gechev et al., 2006; Kwak et al., 2006). NO is also known to act as a signaling intermediate in a variety of responses, such as stomatal guard cell closure, disease resistance, responses to abiotic stresses, and during development in plants (for review, see Delledonne, 2005; Neill et al., 2008).

Both ROS and NO have been implicated in mediating signaling responses in tip-growing cells. Recent data have shown that ROS is involved in regulating polarity and growth in tip-growing cells in plants (Foreman et al., 2003; Monshausen et al., 2007; Potocký et al., 2007; Cárdenas et al., 2008; Coelho et al., 2008). Arabidopsis root hairs exhibit high apical levels of ROS, which is proposed to modulate root hair tip growth by activating a Ca^{2+} channel (Foreman et al., 2003), and a requirement for tip-localized ROS in pollen tube tip growth has been demonstrated (Potocký et al., 2007). NADPH oxidases are implicated in regulating ROS in these systems; AtrbohC (for Arabidopsis [*Arabidopsis thaliana*]-specific respiratory burst oxidase homolog C) is involved in regulating tip growth in root hairs (Monshausen et al., 2007), and ROS produced by a NADPH oxidase are localized as a tip-high gradient in pollen tubes (Potocký et al., 2007; Wang et al., 2010). Transient increases in ROS have been observed in *Phaseolus vulgaris* root hair tips responding to Nod factors (Cárdenas et al., 2008), and disruption of apical ROS in pear (*Pyrus pyrifolia*) pollen was observed during SI (Wang et al., 2010). Thus, substantial data indicate a role for ROS in regulating tip growth, including pollen tubes. Fewer data exist relating to a role for NO signaling in regulating tip growth, but NO has been shown to play a role in regulating pollen tube growth rates and to stimulate reorientation in *Lilium longiflorum* pollen tubes (Prado et al., 2004). Monitoring of ROS and NO in pistils has provided evidence for ROS/NO involvement in signaling during in vivo pollination in Arabidopsis and *Senecio squalidus* (McInnis et al., 2006). Although this study did not show their intracellular localization, a role for ROS and NO in regulating pollen tube growth and pollen-pistil interactions was suggested.

As ROS and NO are such universal signaling molecules and play key roles in many processes, including control of tip growth, pollen-pistil interactions, and also defense signaling, and as there are many analogies between defense signaling and SI, we examined whether there is evidence for ROS or NO in signaling in SI within incompatible *Papaver* pollen. We provide evidence that SI induces relatively rapid and transient increases in ROS and NO, suggesting that they act in a signaling capacity. Moreover, they have distinctive temporal "signatures." We show that Ca^{2+} acts upstream of ROS and NO increases and that ROS and NO signal to mediate both the formation of SI-induced actin punctate foci and the activation of a DEVDase/caspase-3-like activity previously shown to be involved in the execution of SI-PCD. This demonstrates that ROS and NO act upstream of these SI markers and suggests that they signal to these key SI events.

RESULTS

ROS Distribution in Normally Growing *Papaver* Pollen Tubes

We used the ROS probe chloromethyl-2′7′-dichlorodihydrofluorescein diacetate acetyl ester (CM-H_2DCF-DA) to determine the distribution of ROS in normally growing pollen tubes of *Papaver* grown in vitro. This probe is oxidized to fluorescent chloromethyl-2′7′-dichlorofluorescein (CM-DCF) following oxidation by ROS. In normally growing pollen tubes, there was a relatively even fluorescent signal throughout the cytosol, with a slightly speckled appearance (Fig. 1, A and B; $n > 65$). Our observations are similar to those reported in tobacco (*Nicotiana tabacum*) pollen tubes by Potocký et al. (2007). In unlabeled pollen tubes, no fluorescence was detected under the same conditions (data not shown).

To assess the reliability of CM-H_2DCF-DA as a ROS probe, we used hydrogen peroxide (H_2O_2) and diphenyleneiodonium (DPI), an inhibitor of flavin-linked oxidases, including NADPH oxidase. Untreated pollen tubes showed a low, relatively constant signal over the time period of our experiments; addition of 2.5 mM H_2O_2 resulted in an increase in fluorescence (Fig. 1C), demonstrating that the probe detects increases in H_2O_2. Quantification revealed that the largest increase observed was 3.4-fold, with a mean increase of 2.34-fold ± 0.77-fold (SD; $n = 5$). We used DPI to further verify that the CM-H_2DCF-DA detected ROS. Pretreat-

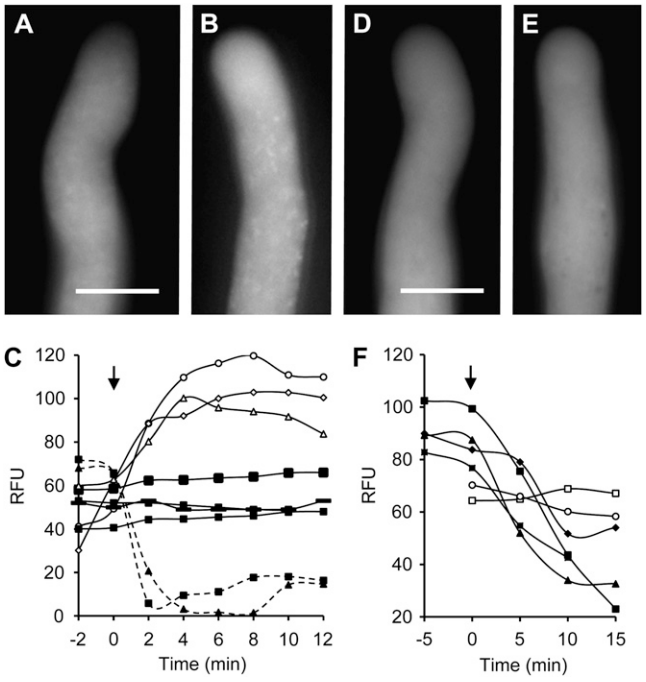

Figure 1. ROS and NO distribution and verification in normally growing *Papaver* pollen tubes. A and B, Typical representative untreated, normally growing *Papaver* pollen tubes labeled with CM-H_2DCF-DA to monitor ROS by formation of fluorescent CM-DCF. Bar = 10 μm. C, Quantification of CM-DCF fluorescence in normally growing untreated pollen tubes (black symbols and solid lines). The signal remains relatively stable over the time course. After addition of 2.5 mM H_2O_2 (arrow), CM-DCF fluorescence (white symbols, solid lines) increased. After addition of 200 μM DPI (arrow), CM-DCF fluorescence decreased (black symbols, dashed lines). Measurements are of relative fluorescence units (RFU) measured in individual pollen tubes. D and E, Typical representative untreated, normally growing *Papaver* pollen tubes labeled with DAF-FM-DA to monitor NO by formation of fluorescent DAF-FM-T. Bar = 10 μm. F, Quantification (in relative fluorescence units) of DAF-FM-T fluorescence in untreated pollen tubes (white symbols) and after addition of 400 μM cPTIO (black symbols).

ment with 200 μM DPI resulted in inhibited pollen tubes with decreased fluorescence (Fig. 1C). The mean decrease in fluorescence observed was 1.94-fold ± 0.25-fold (n = 4). These data support the conclusion that the reactive species measured by the probe are mainly ROS. Since oxidation of the probe is irreversible, the decrease in fluorescence after DPI addition must be caused by diffusion of the probe, allowing visualization of transient ROS production. This phenomenon has previously been observed in *Phaseolus* root hair tips, where a rapid and transient ROS response was observed (Cárdenas et al., 2008). Together with the validated use of CM-H_2DCF-DA in pollen tubes previously (Potocký et al., 2007), these data strongly support the notion that it is ROS being monitored by this probe. Moreover, they strongly suggest that NADPH oxidase is the enzyme responsible for generating most of the ROS signal detected.

NO Distribution in Normally Growing *Papaver* Pollen Tubes

We visualized NO distribution in normally growing *Papaver* pollen tubes using the fluorescent NO probe 4-amino-5-methylamino-2′,7′-difluorofluorescein diacetate (DAF-FM-DA). NO is produced in vivo at very low concentrations, and this, combined with its short half-life (a few seconds) and rapid diffusion in cells, makes imaging using sensitive DAF-based probes the method of choice. DAF has been widely used to detect localized production of NO in plant cells, including pollen tubes (Prado et al., 2004). The membrane-permeable nonfluorescent DAF-FM-DA is nitrosated by an intermediate of NO oxidation to form the fluorescent DAF-FM-triazole (DAF-FM-T). DAF-FM-T fluorescence was generally distributed evenly throughout the pollen tube cytosol (Fig. 1, D and E; $n > 65$).

The NO scavenger 2-(4-carboxyphenyl)-4,4,5,5-tetramethylimidazoline-1-oxyl-3-oxide (cPTIO) has previously been used to provide evidence that DAF reliably reports NO in pollen tubes (Prado et al., 2004). To assess the reliability of the DAF-FM-DA probe, we tested the effect of adding 400 μM cPTIO to pollen tubes labeled with DAF-FM-DA. This resulted in inhibited pollen tube growth and large decreases in fluorescence, probably because of nitrosylated probe diffusion, as discussed earlier. Quantification revealed that while unstimulated pollen tubes showed relatively constant levels of fluorescence, the maximum decrease observed with the addition of cPTIO was 4.5-fold, with a mean decrease of 3.0-fold ± 1.1-fold (n = 4; Fig. 1F). This confirms that this probe detects NO in *Papaver* pollen tubes.

As ROS-NO cross talk is known in other systems (Delledonne et al., 2001; Neill et al., 2002; Zaninotto et al., 2006), we wondered if there was any evidence for interaction between these two signaling molecules in pollen tubes. To examine this, we labeled pollen tubes with the DAF-FM-DA probe, added 2.5 mM H_2O_2 to increase ROS, and monitored the consequent effect of this on DAF-FM-T fluorescence. The NO probe signal was detectable in untreated pollen tubes (Fig. 2A), and the level of fluorescence significantly increased when H_2O_2 was added (Fig. 2B). As H_2O_2 stimulated increases in the DAF-FM-T signal, this suggests that increases in ROS can stimulate increases in NO, implicating cross talk between ROS and NO. To further assess this, we investigated whether using the NADPH oxidase inhibitor DPI to inhibit ROS might lower NO levels. Growing pollen tubes were labeled with DAF-FM-DA, and addition of DPI resulted in a decrease in DAF-FM-T fluorescence (Fig. 2, C and D; n = 5). As decreasing ROS resulted in reductions in NO in these pollen tubes, this provides further evidence for cross talk between ROS and NO. However, we cannot rule out the possibility of cross-reactivity of the probe with reactive nitrogen species. Quantification (Fig. 2E) showed that increases in DAF-FM-T signal stimulated by the addition of H_2O_2 were large; the

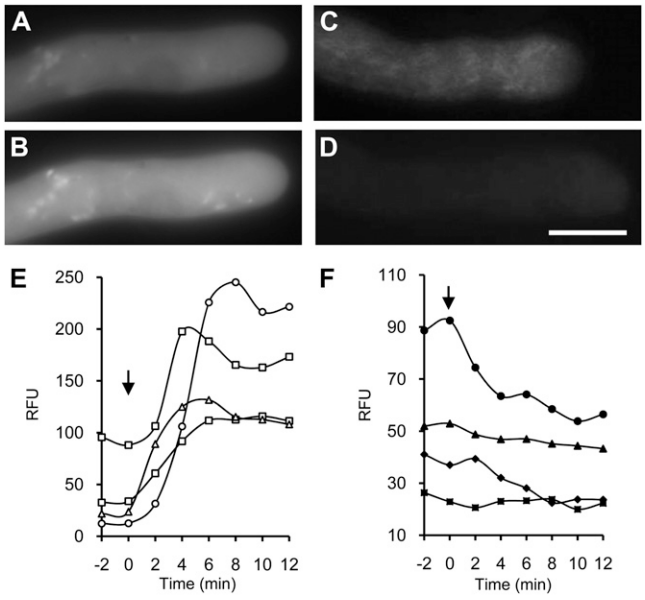

Figure 2. Evidence for ROS-NO cross talk in normally growing pollen tubes. A and B, Representative pollen tube labeled using DAF-FM-DA to form fluorescent DAF-FM-T (A) and DAF-FM-T signal 4 min after addition of 2.5 mM H_2O_2 (B). C and D, Representative pollen tubes labeled as in A (C) and DAF-FM-T signal 5 min after addition of 200 μM DPI (D). Bar = 10 μm for A to D. E and F, Quantification (in relative fluorescence units [RFU]) of DAF-FM-T fluorescence after addition of 2.5 mM H_2O_2 (E) and after addition of 200 μM DPI (F) at time zero (arrows).

largest increase observed was 18.1-fold; the mean increase was 7.4-fold ± 7.3-fold (n = 4). The decrease in DAF-FM-T signal after adding DPI, which inhibits NADPH oxidase, was relatively small (Fig. 2F). The largest decrease in signal was 2.5-fold, with a mean decrease of 2.0-fold ± 0.58-fold (n = 4). Again, one might expect a decrease in fluorescence intensity due to diffusion or cytoplasmic streaming diluting the dye signal; this would be countered if NO production continued, so it suggests that DPI inhibits net NO production under these conditions.

SI Stimulates Increases in ROS in Incompatible *Papaver* Pollen Tubes

Having established that pollen tubes normally exhibit relatively steady levels of ROS (Fig. 1C), we wished to determine whether SI induced alterations in ROS levels. SI was induced in pollen tubes labeled with CM-H_2DCF-DA by the addition of incompatible recombinant PrsS (see "Materials and Methods") and ROS levels were monitored using fluorescence microscopy. SI stimulated large increases in ROS (Fig. 3; n = 21). In many cases, the increases were rapid, peaking at 4 to 5 min (Fig. 3, A and B); in others, there was a lag of approximately 5 to 6 min (Fig. 3, C–E), after which the ROS signal rapidly increased (Fig. 3F), peaking at approximately 12 min (Fig. 3G). The fluorescence subsequently decreased (Fig. 3, H and I), indicating that the elevations in ROS were relatively small and transient. Although this reduction in signal was unexpected, as oxidation makes the probe irreversibly fluorescent, the most likely explanation is that this is due to redistribution of the fluorescent probe throughout the pollen tube (presumably as a result of diffusion), as we did not see any signs of sequestration and we did not see any major reorganization of the organelles within this time period (Fig. 3J). The increases in ROS were detected throughout the shank of the pollen tube. This provides evidence for cytosolic ROS, as there was considerable diffuse fluorescence; there were also many small fluorescence "hot spots" (Fig. 3, B and F–H), and there appeared to be movement of these hot spots (Supplemental Movies S1 and S2). While these hot spots of ROS production resemble mitochondria (visualized using MitoTracker MT-CMXRos in *Papaver* pollen tubes [Bosch et al., 2010]), ascertaining whether the SI-induced ROS hot spots correspond to mitochondria is problematic, as mitochondrial integrity is affected by the SI response (Thomas and Franklin-Tong, 2004; K.A. Wilkins, M. Bosch, and V.E. Franklin-Tong, unpublished data). Untreated, control pollen tubes did not exhibit this increase in fluorescence over a similar time frame, and unlike SI-induced samples, pollen tubes continued to grow (Supplemental Movie S3). Although these increases in ROS concentration appear large, a sensitive CCD camera was required to detect these increases, suggesting that SI stimulates relatively small increases in ROS. Quantitative analysis of the SI-induced alterations in CM-DCF signal, indicating ROS, revealed that the temporal response was usually quite rapid (Fig. 3K). Often, the signal peaked at approximately 3 to 6 min (n = 4), after which the signal returned to basal levels by approximately 10 to 15 min, although some responses were delayed, peaking at approximately 20 min, with basal levels achieved between 15 and 30 min. Quantification revealed that the largest increase was 6.7-fold, with a mean increase of 3.67-fold ± 2.03-fold (n = 6) in the shank region. Control, growing pollen tubes exhibited no such increases over these time periods (Figure 3K).

We also investigated whether pretreatment with DPI prior to SI induction affected the SI-induced increases in ROS. In all cases, the SI-induced increases attributed to ROS were inhibited by 100 μM DPI (n = 5), while controls without DPI were not (Supplemental Fig. S1). Together, these data provide good evidence that SI triggers relatively rapid and transient increases in ROS, suggesting a signaling role for ROS in SI. Moreover, as DPI inhibits the signal, this implicates NADPH oxidases in the generation of the SI-stimulated ROS.

SI Stimulates Increases in NO in Incompatible *Papaver* Pollen Tubes

To determine whether SI might also involve alterations in NO, pollen tubes were labeled with DAF-FM-

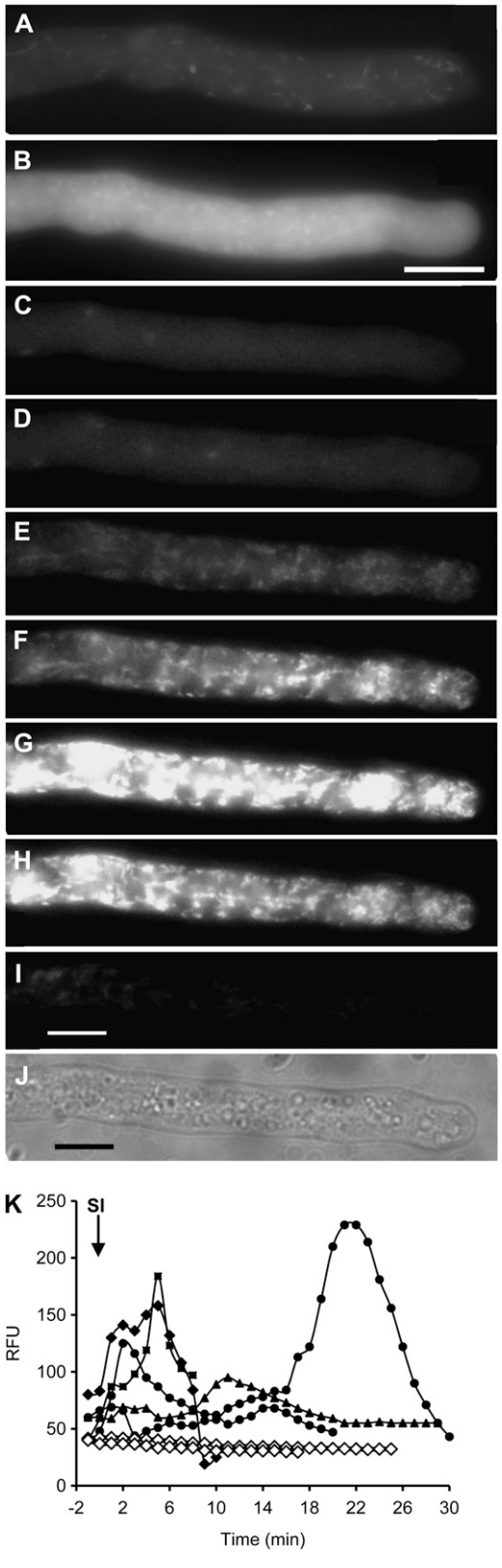

Figure 3. SI stimulates increases in ROS in incompatible pollen tubes. A, Normally growing pollen tube labeled with CM-H_2DCF-DA to monitor ROS by formation of fluorescent CM-DCF 1 min after SI induction. B, The same pollen tube 4 min after SI induction. C, CM-DCF fluorescence in a growing pollen tube before SI induction. D to I, The same pollen tube 2 min after SI induction (D) and 7 min (E), 9 min (F), 12 min (G), 14 min (H), and 20 min (I) after SI induction. J, Bright-field image at the end of the series. Bars = 10 μm. K, Representative examples of quantitation of CM-DCF in untreated pollen tube (white symbols) and after SI challenge induced at time zero (arrow; black symbols). Measurements are of relative fluorescence units (RFU) measured in individual pollen tubes.

DA, subjected to SI induction, and NO levels monitored using fluorescence microscopy. In contrast to the relatively rapid increases in ROS stimulated by SI, NO levels remained constant for a considerable time after SI induction. Figure 4 shows typical examples of the localization of SI-induced increases in NO observed in two representative pollen tubes. Unchallenged pollen tubes displayed a relatively low DAF-FM-T signal throughout the pollen tube shank (Fig. 4A; see also Fig. 1C). After SI induction, large increases in the levels of DAF-FM-T fluorescence were observed (n = 36). The signal was primarily in the cytosol, but there were also hot spots of localized high fluorescence, giving a speckled/reticulate appearance, which increased over time as the signal increased (Fig. 4, B–F). Untreated pollen tubes examined over a similar time course did not exhibit these distinctive increases in fluorescence, and pollen tubes continued to grow (Fig. 4, G–J; Supplemental Movie S4). Like the ROS signals, there was distinctive movement of the SI-stimulated hot spots (Supplemental Movies S5 and S6). The spatial localization of the increases in NO increased throughout the shank. The temporal pattern of the SI-induced NO was slow and was consistently preceded by a lag phase of approximately 10 to 20 min (Fig. 4K). The fluorescence consistently increased gradually and often took more than 20 min to peak (Fig. 4, B–E and K). The fluorescence subsequently decreased (Fig. 4, F and K), which is unexpected, as the nitrosated probe is nonreversibly fluorescent. Thus, our data suggest that the NO signal (like the ROS signal) is sufficiently small to be redistributed throughout the pollen tube, resulting in an overall reduction in levels.

Quantification of the increases in fluorescence attributed to NO revealed that the largest increase measured was 7.1-fold, with a mean increase of 3.34-fold $\pm$ 2.19-fold (n = 6) for the overall shank region. Regardless of why the signal drops, these data provide clear evidence that SI stimulates transient increases in NO, suggesting a signaling role for NO in SI. Moreover, the SI-induced changes in fluorescence intensity using CM-H_2DCF-DA and DAF-FM-DA (Figs. 3K and 4K) show that they are temporally quite distinct, indicating that the probes are reporting different events.

Increases in $[Ca^{2+}]_{cyt}$ Stimulate Increases in ROS and NO in *Papaver* Pollen Tubes

As increases in $[Ca^{2+}]_{cyt}$ are triggered by SI, we wished to ascertain whether ROS and NO increases

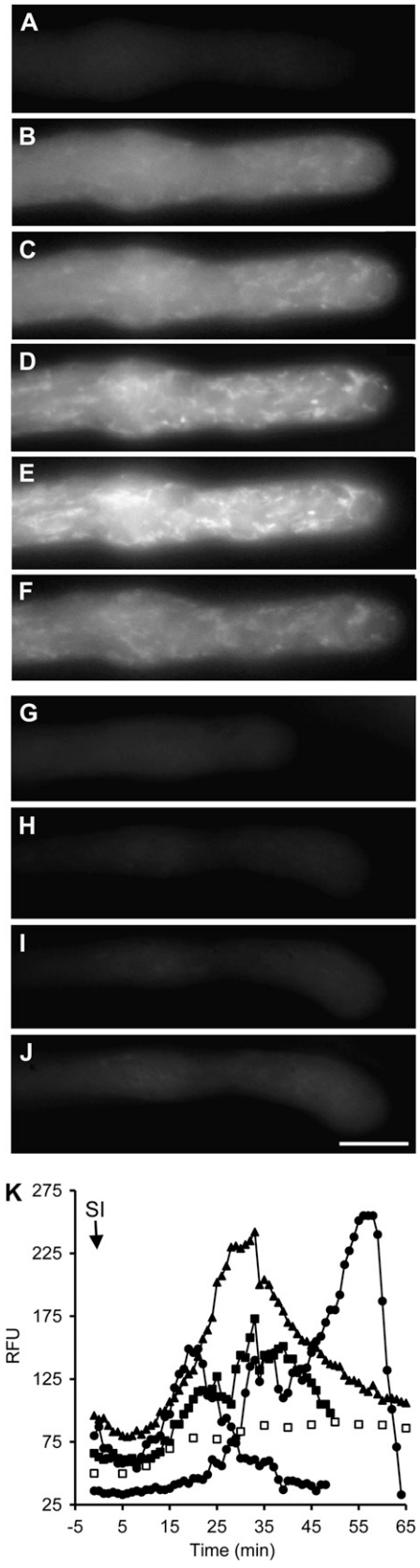

Figure 4. SI stimulates increases in NO in incompatible pollen tubes. Pollen tubes were labeled with DAF-FM-DA. A to F, Typical DAF-FM-T signal in a pollen tube imaged after SI induction. Images are before SI induction (A) and 23 min (B), 27 min (C), 31 min (D), 53 min (E), and 63 min (F) after SI. G to J, Typical DAF-FM-T signal in an untreated pollen tube imaged for a similar time series. Images are at 0 min (G), 24 min (H), 34 min (I), and 45 min (J). Bar = 10 μm. K, Representative examples of quantitation of DAF-FM-T fluorescence in an untreated pollen tube (white symbols) and after SI challenge (arrow; black symbols). Measurements are of relative fluorescence units (RFU) measured in individual pollen tubes.

were downstream of this very early event. We used the ionophore A23187 to artificially increase $[Ca^{2+}]_{cyt}$ in pollen tubes labeled with CM-H_2DCF-DA and DAF-FM-DA. There was an increase in fluorescence (208%; $P = 0.047$; $n = 13$) in CM-H_2DCF-DA-labeled pollen tubes 20 min after the addition of 10 μM A23187 (Fig. 5A). Similarly, when we added 10 μM A23187 to pollen tubes labeled with DAF-FM-DA, we detected a significant increase in fluorescence (189%) compared with untreated pollen tubes, 23 min after addition (Fig. 5B; $P = 0.003$; $n = 17$). This provides good evidence that increases in $[Ca^{2+}]_{cyt}$ can trigger both increases in ROS and NO, suggesting that they are downstream of SI-induced Ca^{2+} signals.

To verify this, we used 500 μM La^{3+} to block Ca^{2+} influx stimulated by SI (Franklin-Tong et al., 2002). La^{3+} alone did not significantly alter ROS and NO levels in pollen tubes compared with untreated samples (for ROS, $P = 0.0832$; for NO, $P = 0.391$; both nonsignificant). SI triggered an increase in fluorescence attributable to both ROS (Fig. 5C) and NO (Fig. 5D), 671% and 191%, respectively, at 20 and 23 min after SI, compared with untreated pollen tubes ($n = 10$ each). Both were significantly different from untreated levels (for ROS, $P = 0.005$; for NO, $P = 0.0003$). In both cases, no significant increase in ROS or NO was detected after SI in the presence of La^{3+} (Fig. 5, C and D; $P = 0.580$ and $P = 0.884$, respectively; $n = 10$ each) compared with untreated samples. The levels of ROS and NO induced by SI in the presence of La^{3+} were significantly different from the untreated samples ($P = 0.005$ and $P = 7.13 \times 10^{-6}$; $n = 10$ each). This provides evidence that SI-induced ROS and NO are dependent on Ca^{2+} influx.

ROS and NO Signal to SI-Induced Activation of a DEVDase

As SI triggers several key downstream signaling events, we wished to ascertain whether ROS or NO might signal to these diagnostic features of SI in *Papaver*. In order to examine whether ROS or NO was implicated in signaling to PCD, we analyzed the effect of using ROS and NO scavengers on the SI-induced caspase-3-like/DEVDase activity. We pretreated pollen tubes with either the NADPH oxidase inhibitor DPI or the NO scavenger cPTIO and then stimulated SI. Extracts were made after 5 h, when maximal DEVDase activity was exhibited (Bosch and

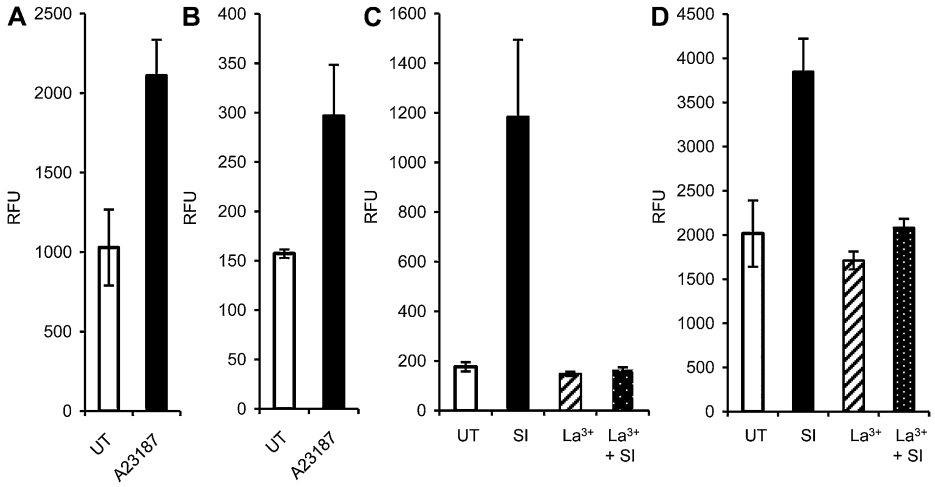

Figure 5. Ca^{2+} is upstream of increases in ROS and NO in *Papaver* pollen tubes. Pollen tubes were labeled with either 2 μM CM-H_2DCF-DA to monitor ROS by formation of fluorescent CM-DCF (A and C) or with 10 μM DAF-FM-DA to monitor NO by formation of fluorescent DAF-FM-T (B and D). Relative fluorescence units (RFU) were measured in normally growing, untreated (UT) pollen tubes (which acted as controls) and after additions, as described. A, CM-DCF fluorescence levels in untreated pollen tubes and 20 min after addition of 10 μM A23187 ($n = 13$). B, Fluorescence levels of DAF-FM-T in untreated pollen tubes and 23 min after addition of 10 μM A23187 ($n = 17$). C, CM-DCF fluorescence levels in untreated pollen tubes, after addition of 500 mM La^{3+}, after SI induction, and 20 min after SI induction in the presence of 500 mM La^{3+} ($n = 10$). D, Fluorescence levels of DAF-FM-T in untreated pollen tubes, after addition of 500 mM La^{3+}, after SI induction, and 23 min after SI induction in the presence of 500 mM La^{3+} ($n = 10$).

Franklin-Tong, 2007), and DEVDase activities were measured (Fig. 6). Pollen showed a slight increase in DEVDase activity of 33% with cPTIO ($P = 0.003$) and a 52% increase with DPI ($P = 0.08$; nonsignificant). An increase of 67% with cPTIO and DPI combined was not significantly different from samples treated with the scavengers individually ($P = 0.17$ and $P = 0.67$). SI resulted in a significant (131%; $P = 5.43 \times 10^{-5}$) increase in DEVDase activity over levels in untreated pollen extracts. When SI was induced in the presence of DPI or cPTIO, DEVDase activity was slightly (but not significantly) reduced compared with SI ($P = 0.214$ and $P = 0.150$), but if SI was induced in the presence of both scavengers, the DEVDase activity was significantly reduced by 119% ($P = 0.001$; Fig. 6) to a level that was not significantly different from untreated samples ($P = 0.671$). All these DEVDase activities were significantly inhibited by the DEVDase inhibitor Ac-DEVD-CHO, verifying that this is an authentic DEVDase activity (Supplemental Fig. S2). As a combination of both scavengers was required to significantly reduce the SI-induced DEVDase activity, this suggests that ROS and NO act in concert or tandem to signal to activate SI-induced PCD through the activation of a DEVDase activity.

ROS and NO Signal to SI-Stimulated Formation of Actin Punctate Foci

A striking SI marker is the formation of punctate actin foci (Poulter et al., 2011), and we wished to examine a possible role for ROS or NO in signaling to the actin cytoskeleton. The typical normal actin configuration in a pollen tube (Fig. 7A) is very different from that in a pollen tube after SI (Fig. 7B; Poulter et al., 2011). Pollen tubes were pretreated with ROS or NO scavengers, and SI was induced. Pollen was examined for the formation of punctate actin foci after 3 h. The NADPH oxidase inhibitor DPI caused altered actin configuration and could not be used for this study, so we used the ROS scavenger TEMPOL, which did not have this effect. cPTIO also did not affect actin organization. We then examined whether the actin in pollen was altered if SI was stimulated after pretreatment with these ROS and NO scavengers.

Quantification of the number of pollen tubes that exhibited punctate actin foci (Fig. 7C), revealed that untreated pollen tubes had virtually no foci (1.5%), while SI treatment resulted in 79% of the tubes containing foci, which was significantly different from untreated tubes ($P = 2.704 \times 10^{-6}$; $n = 70$). Scoring for actin foci, none of the drug treatments alone was significantly different from untreated pollen ($P = 0.507$; $n = 240$). However, when pollen was pretreated with TEMPOL with SI induction, there were significantly less foci than with SI induction alone (35%; $P = 0.023$; $n = 70$). With the addition of cPTIO in the presence of SI, there was a 23% reduction in the number of tubes exhibiting foci, which was significantly different from that for the SI treatment alone ($P = 0.0017$; $n = 70$). When both TEMPOL and cPTIO were added in the presence of SI induction, the occurrence of punctate actin foci was reduced by 38%, which was significantly different from that with SI

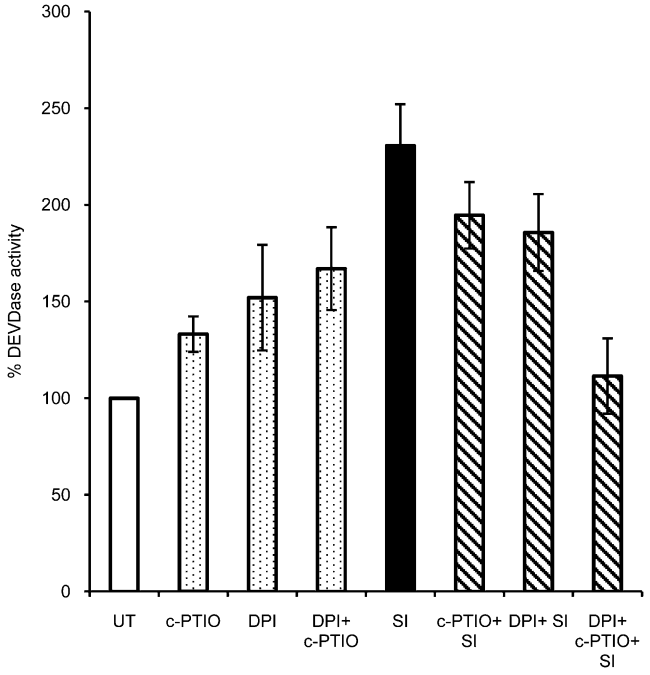

Figure 6. ROS and NO signals to the SI-induced DEVDase activity in pollen. DEVDase activity in *Papaver* pollen extracts were measured using Ac-DEVD-AMC. The levels of DEVDase activity in untreated (UT) samples were compared with those in pollen pretreated with the NO scavenger cPTIO and the NADPH inhibitor DPI, with these inhibitors combined (dotted bars), with levels after SI induction (black bar), and with SI in combination with inhibitor pretreatments (cross-hatched bars). DEVDase activity was calculated as a percentage of untreated activity (assigned 100%), and activities are shown relative to this. Data are means ± SE of five independent experiments.

alone ($P = 0.0032$; $n = 70$). Together, these data suggest that both ROS and NO increases contribute to the signaling events that mediate the formation of the punctate actin foci that are so characteristic of the SI response in incompatible *Papaver* pollen.

DISCUSSION

ROS and NO are highly reactive and diffusible molecules, and they are known to play key signaling roles in both animal and plant cells, regulating many physiological responses. Here, we have used live-cell imaging to demonstrate that induction of SI by the addition of a recombinant protein, PrsS, to incompatible *Papaver* pollen stimulates transient increases in both ROS and NO in response to SI in incompatible pollen. These data describe a physiologically relevant, defined protein ligand stimulus-induced ROS/NO response in pollen tubes and suggest an involvement for both ROS and NO in the SI-mediated PCD-signaling network. They represent, to our knowledge, the first steps in investigating ROS/NO signaling triggered by receptor-ligand interactions in pollen tubes.

Temporal-Spatial Pattern of ROS and NO Signaling in the SI Response

Few studies have examined ROS or NO in pollen tubes in response to physiologically relevant signals, although it has been shown that an external source of NO stimulates pollen tube reorientation (Prado et al., 2004) and that S-RNase disrupts tip-localized ROS in incompatible *Pyrus* pollen tubes (Wang et al., 2010). Although transient increases in ROS have been reported as being tip localized in root hairs of *Phaseolus* responding to Nod factors (Cárdenas et al., 2008), the spatial localization that we have observed here in the shank of the pollen tube is quite different. This supports the concept that distinct spatial-temporal signatures of common signaling compounds generate signal specificity (Knight et al., 1996; Rudd and Franklin-Tong, 1999; Foyer and Noctor, 2005). The origin of the ROS requires further investigation. Sensitivity to DPI inhibition is often taken as evidence for the involve-

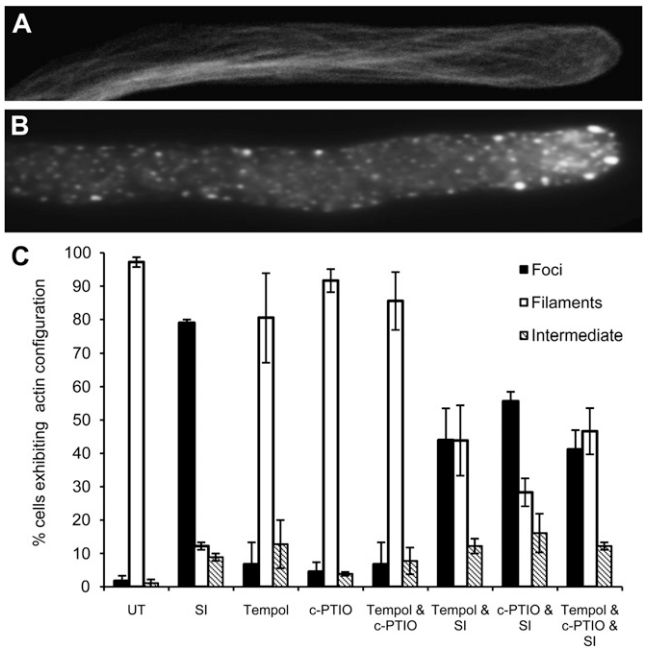

Figure 7. ROS and NO signal to SI-stimulated formation of actin punctate foci. Pollen tubes were pretreated with ROS or NO scavengers, SI was induced, and F-actin was stained using rhodamine-phalloidin and examined with fluorescence microscopy. A and B, Typical representative images of actin configuration in a control pollen tube (scored as "filaments" [A] in C) and 3 h after SI showing punctate actin foci (scored as "foci" [B] in C) C, Quantification of the effect of pretreatment of pollen with the ROS scavenger TEMPOL, the NO scavenger cPTIO, and both TEMPOL and cPTIO together prior to SI induction on F-actin configuration. Actin configuration was assessed using fluorescence microscopy of rhodamine-phalloidin staining, placing each pollen tube into one of three categories: normal (A), punctate foci (B), or intermediate (i.e. somewhere in between). Three independent experiments scored 70 pollen tubes in total for each treatment, and the percentage of pollen tubes in each category is indicated. Error bars indicate SE, based on the average percentage values.

ment of the plasma membrane-localized NADPH oxidases in generating superoxide and H_2O_2. These enzymes are involved in pollen tube and root hair growth (Foreman et al., 2003; Potocký et al., 2007), the hypersensitive response (Torres et al., 2002), and abscisic acid-induced stomatal closure (Kwak et al., 2003). However, our data suggest that the source of SI-stimulated ROS is different, as tip growth is NADPH oxidase dependent and apically localized NADPH oxidases will be rapidly inhibited concomitant with SI-induced inhibition of growth, and we see SI-induced increases at localities that cannot be at the plasma membrane. In support of this proposal, the DPI inhibition of SI-stimulated ROS could result from inhibition of mitochondrial ROS production, as in animal cells (Li and Trush, 1998). Superoxide-generating enzymes such as peroxidase are also inhibited by DPI (Frahry and Schopfer, 1998), so their involvement in the SI response cannot be ruled out. There are many ROS-scavenging enzymes that could ensure that the increases are transient and regulated. Increasing evidence suggests that they interact with ROS to modulate signaling to physiological responses, including PCD (Mittler et al., 2004; Foyer and Noctor, 2005). It is currently unclear which enzymes may be implicated in NO production in plants (for a recent review, see Moreau et al., 2010) . Our studies represent, to our knowledge, the first steps in uncovering the temporal characteristics of a physiologically relevant ROS signal involved in receptor-ligand interactions in pollen tubes. They add to data suggesting that the ROS (and probably also NO) signatures associated with the perception of different interactions in tip-growing systems are likely to be distinct to mediate different responses.

Evidence for Cross Talk between Ca^{2+}, ROS, and NO in *Papaver* Pollen Tubes

There is evidence for cross talk between $[Ca^{2+}]_{cyt}$ and ROS and NO in other systems (Besson-Bard et al., 2008; Courtois et al., 2008). The tip-high $[Ca^{2+}]_{cyt}$ gradient characteristic of tip-growing cells is closely associated with NADPH oxidase generation of ROS in pollen tubes (Potocký et al., 2007) and root hairs (Foreman et al., 2003), suggesting that $[Ca^{2+}]_{cyt}$ may be responsible for stimulating increases in ROS. The localization of ROS and NO in the pollen tube shank described here is reminiscent of the SI-induced $[Ca^{2+}]_{cyt}$ wave observed in earlier studies (Franklin-Tong et al., 1993, 1997). In the SI system, the ROS and NO signals temporally lag behind the $[Ca^{2+}]_{cyt}$ signals, as SI stimulates virtually instantaneous increases in $[Ca^{2+}]_{cyt}$ (Franklin-Tong et al., 1993, 1997) and Ca^{2+} influx (Wu et al., 2011). Increases in Ca^{2+} can trigger increases in ROS and NO levels in other systems (Wendehenne et al., 2004; Potocký et al., 2007; Besson-Bard et al., 2008; Coelho et al., 2008). As NADPH oxidases possess EF-hand motifs (Sagi and Fluhr, 2001; Bánfi et al., 2004), Ca^{2+} can regulate NADPH oxidase activity and thus ROS production (Torres et al., 1998). Here, we have shown that ROS and NO in *Papaver* pollen tubes are downstream of, and dependent on, $[Ca^{2+}]_{cyt}$; ROS and NO increased if $[Ca^{2+}]_{cyt}$ was artificially raised, and blocking increases in SI-stimulated $[Ca^{2+}]_{cyt}$ resulted in no increases in ROS or NO.

The temporal separation of increases in ROS and NO, where the ROS transient has peaked and declined before NO starts to increase, makes it tempting to speculate that cross talk might occur between ROS and NO signaling during SI. ROS-NO cross talk has been observed in several other plant systems, in particular in relation to signaling to PCD (Neill et al., 2002; Zaninotto et al., 2006). Moreover, evidence for cross talk between ROS and NO has been observed in vivo in pollinated stigmas of *Senecio*, where evidence that increasing pistil NO levels can result in a reduction in ROS levels in pollen tubes was provided; interactions between germinating pollen grains and stigmatic papillae also resulted in reduced pistil ROS/H_2O_2 (McInnis et al., 2006). However, as NO increases occur after ROS decreases in the SI response, the response is clearly different.

Evidence for ROS and NO Signaling to SI-Induced Actin Foci in *Papaver* Pollen

How ROS and NO signaling integrate into the known SI signaling network is important. We investigated whether the increases in ROS and NO might signal the formation of the SI-induced actin foci, which are a characteristic feature of the SI response (Geitmann et al., 2000; Snowman et al., 2002; Poulter et al., 2010). ROS signaling to actin aggregation has been documented in yeast (Franklin-Tong and Gourlay, 2008). There is strong evidence that elevations in ROS can signal to actin polymerization in animal cells. ROS signals to mediate actin dynamics responsible for cytoskeletal reorganization in animal endothelial cells. Actin polymerization was stimulated in the presence of free radicals, and artificially decreasing ROS using DPI strongly inhibited actin monomer incorporation at the fast-growing barbed ends of filaments (Moldovan et al., 2000). The reorganization of actin microfilaments stimulated by increases in ROS suggests that it is an early target for oxidative stress (Dalle-Donne et al., 2001). Interestingly, heat shock proteins, which have recently been found to be associated with the SI-induced actin foci (Poulter et al., 2011), are implicated in oxidative stress-induced F-actin reorganization in animal cells and are mediated by a MAPK signaling pathway (Dalle-Donne et al., 2001). Here, we show that the formation of SI-stimulated F-actin foci, which are highly stable (Poulter et al., 2010), is significantly inhibited by the ROS scavenger TEMPOL. This suggests that ROS may also play a role in influencing actin polymerization dynamics in plant cells. Investigating whether the SI-induced p56-MAPK (Rudd et al., 2003; Li et al., 2007) is also involved in signaling to this network should clearly be investigated in the future.

NO signaling to alterations in F-actin organization has been observed in mammalian cells. For example, chondrocytes treated with exogenous NO formed short, rod-like structures of polymerized actin (Frenkel et al., 1996). This appears to be rather similar to what we observed in *Papaver* SI. There are virtually no data on NO signaling to actin in plant cells. Proteomic studies in Arabidopsis identified nitrosylated proteins, including actin (Lindermayr et al., 2005). Thus, actin may be a target for NO signals. NO is well established to modify proteins by *S*-nitrosylation. Importantly, it has been shown that nitrosylation of a single Cys residue on mammalian actin can alter actin dynamics in vitro (Dalle-Donne et al., 2000). Moreover, alterations in actin organization have recently been observed in maize (*Zea mays*) roots treated with the NO donor SNAP (Kasprowicz et al., 2009).

Evidence for ROS and NO Signaling to SI-Induced PCD in *Papaver* Pollen Tubes

As PCD is triggered in incompatible pollen (Thomas and Franklin-Tong, 2004; Bosch and Franklin-Tong, 2007) and ROS-NO signaling is known to participate in PCD signaling networks (Foyer and Noctor, 2005; van Breusegem and Dat, 2006), we investigated whether the increases in ROS and NO might signal to SI-induced PCD. It is well established that ROS can signal to trigger defense-mediated PCD. The intracellular redox balance is known to be critical, and altering levels of antioxidants results in PCD (Mittler et al., 2004). Thus, it is not surprising that ROS participate in SI-mediated PCD. Interfering with ROS or ROS and NO production in pollen tubes resulted in increased levels of a DEVDase/caspase-3-like activity. This fits with the idea of intracellular ROS and NO homeostasis being important for "health" status. Importantly, preventing/reducing increases in both ROS and NO (but not each individually) triggered during SI induction prevented DEVDase activation. This suggests that ROS and NO signal in concert/tandem to initiate SI-mediated PCD. As mentioned earlier, both ROS and NO are known to signal to PCD (Neill et al., 2002; Zago et al., 2006; Zaninotto et al., 2006), and it is well established that NO and H_2O_2 operate in partnership during the hypersensitive response (Delledonne et al., 2001; de Pinto et al., 2002).

Establishing that both ROS and NO mediate downstream SI signals to PCD is an important step in gaining a fuller picture of how SI signaling is integrated. It is currently thought that NO signaling in plants uses *S*-nitrosylation of Cys residues of redox-sensitive proteins (Wang et al., 2006; Moreau et al., 2010). How, exactly, ROS and NO signal to PCD is an important question for the future. One possibility is that actin may be involved. The role of NO in actin stabilization-mediated apoptosis has been demonstrated in chondrocytes. Stabilizing actin filaments with jasplakinolide caused aggregation of F-actin and enhanced NO-induced apoptosis, while depolymerization resulted in the inhibition of NO-induced apoptosis in chondrocytes (Kim et al., 2003). Despite the known sensitivity of the actin cytoskeleton to ROS and NO, the mechanisms utilized to alter the dynamics and organization of actin filaments is far from clear, even in animal cell systems. Here, we have made, to our knowledge, the first steps in beginning to understand how this may be mediated in plant cells.

In summary, we show here that SI in *Papaver* pollen stimulates increases in both ROS and NO. Although ROS and NO distribution have been described in normally growing pollen tubes and other tip-growing cells, such as root hairs and polarizing algae, our study involves a biologically relevant stimulus-induced ROS/NO response in pollen tubes triggered by a specific receptor-ligand interaction in pollen tubes. The rapidity of the ROS and NO responses suggests that they act in a signaling capacity and contribute to mediate key events induced by SI, including the formation of punctate actin foci and the activation of a DEVDase/caspase-3-like protease. To our knowledge, this represents the first steps in understanding ROS/NO signaling triggered by this receptor-ligand interaction and how these signals integrate with other components in the SI-induced signaling network in pollen tubes (Supplemental Fig. S3).

MATERIALS AND METHODS

Pollen Tube Growth and Labeling with Fluorescent Probes

Pollen of *Papaver rhoeas* (the field poppy) was germinated and grown in vitro in liquid growth medium [GM; 0.01% H_3BO_3, 0.01% KNO_3, 0.01% $Mg(NO_3)_2.6H_2O$, 0.036% $CaCl_2.2H_2O$, and 13.5% Suc] as described previously (Snowman et al., 2002). Pollen grains were suspended in liquid GM and added to a 35-mm petri dish with a thin layer of GM solidified with 1.2% agarose. Pollen tubes were grown for 45 min at 28°C prior to being labeled with cell-permeable probes.

CM-H_2DCF-DA (2 μM; Invitrogen) was used for ROS visualization. CM-H_2DCF-DA is membrane permeable and, once taken up, is hydrolyzed to CM-H_2DCF by intracellular esterases. CM-H_2DCF reacts rapidly with hydroxyl radicals and peroxynitrite and also reacts well with H_2O_2 as long as peroxidase is present (Hempel et al., 1999; Halliwell and Whiteman, 2004) to form fluorescent CM-DCF. It also reacts with superoxide and NO, but at a slower rate compared with the other oxidants (Halliwell and Whiteman, 2004). Therefore, CM-H_2DCF-DA can be used as a general probe for ROS with relatively low affinity for NO. Despite its lack of specificity, the general consensus is that it indicates ROS production in plant cells, including tip-growing cells such as roots and pollen tubes (Foreman et al., 2003; Riganti et al., 2004; Shin and Schachtman, 2004; McInnis et al., 2006; Yao and Greenberg, 2006; Potocký et al., 2007; Van Breusegem et al., 2008).

DAF-FM-DA (10 μM; Invitrogen) was used for NO detection. This probe is designed for real-time detection of NO in living cells forming a fluorescent benzotriazole derivative, DAF-FM-T. Oxidized forms of NO such as NO_2^- and NO_3^- and reactive oxygen species (e.g. $O_2^{\cdot -}$, H_2O_2, peroxynitrite) do not react with DAF-2 to give a fluorescent product. Interference from other nonspecific reactions (Balcerczyk et al., 2005; Planchet and Kaiser, 2006; Wardman, 2007) can be mitigated with suitable controls such as the NO scavenger cPTIO.

The probes were added to pregrown pollen tubes and left in the dark for 30 min (CM-H_2DCF-DA) and 10 min (DAF-FM-DA) to label pollen tubes. After labeling, pollen tubes were resuspended in 500 μL of GM. For imaging, labeled cells were pipetted onto 35-mm glass-bottom microwell culture dishes with a No. 1.5 coverglass (MatTek), coated with 0.001% (w/v) poly-L-Lys, and covered with a thin layer of GM. After leaving to adhere for 2 min, the GM was replaced with fresh GM. Pollen tubes were imaged, either immediately in untreated pollen tubes or after treatments (see below). Only growing labeled

pollen tubes were imaged; the growth rate was normally approximately 3 to 6 μm min^{-1}.

Treatments

Final concentrations of treatments were as follows: DPI, 200 μM; cPTIO, 400 μM, and H_2O_2, 2.5 mM. Treatments were performed on prelabeled pollen tubes growing in 35-mm glass-bottom microwell culture dishes and imaged immediately afterward.

For SI treatments, recombinant pistil PrsS proteins were produced by expressing and purifying the nucleotide sequences specifying the mature peptide of the $PrsS_1$ and $PrsS_3$ alleles of the *S* gene (pPRS100 and pPRS300) as described previously (Foote et al., 1994; Kakeda et al., 1998). SI was induced by adding recombinant PrsS (final concentration, 15 μg mL^{-1}) to pollen of the appropriate *S*-haplotype to generate an incompatible combination (e.g. $PrsS_1$ and $PrsS_3$ with pollen from plants of haplotype S_1S_3; Snowman et al., 2002; Wheeler et al., 2009) growing in vitro as described earlier.

For SI induction with DPI pretreatment, CM-H_2DCF-DA-labeled pollen tubes were pretreated with DPI 10 min prior to SI induction. SI-positive controls were carried out at the same time, using the same batch of PrsS to check that pollen tubes were responsive in the absence of DPI. For SI induction with La^{3+}, pollen tubes labeled with CM-H_2DCF-DA and DAF-FM-DA were subjected to SI in the presence of 500 μM La^{3+}. For SI induction in the presence of ROS and NO scavengers, labeled pollen tubes were pretreated with the ROS scavenger TEMPOL (2 mM) or DPI (400 μM) or the NO scavenger cPTIO (200 μM), pretreated for 10 min, and SI was induced. For treatments with the ionophore A23187, pollen tubes were labeled with either CM-H_2DCF-DA and DAF-FM-DA. Images were taken from untreated samples and from samples after 10 μM A23187 was added.

Visualization of F-Actin in Pollen Tubes

Pollen tubes were fixed in 400 μM 3-maleimodobenzoic acid *N*-hydroxysuccinimide ester (Pierce) for 6 min followed by 2% formaldehyde (1 h, 4°C). Pollen tubes were washed in TBS (50 mM Tris, pH 7.6, and 200 mM NaCl) and then permeabilized with TBS + 0.1% Triton X-100 for 15 min. F-actin was labeled by the addition of 66 nM rhodamine-phalloidin (Invitrogen) overnight at 4°C, then pollen tubes were mounted on slides with 5 μL of Vectashield + 4′,6-diamino-phenylindole (Vector Laboratories) and imaged using fluorescence microscopy.

Microscopy

All fluorescent images of pollen labeled using CM-H_2DCF-DA and DAF-FM-DA were captured using a Nikon Eclipse TE-300 microscope with a 60× or a 100× Plan Apo Nikon oil-immersion objective (1.4 numerical aperture), a fluorescein isothiocyanate filter (excitation, 492 nm; Chroma Technology), and a Nikon DS-Qi1MC monochrome cooled CCD camera with Nikon NIS elements software. All signals were very low, as expected for physiologically relevant signals. To ensure that images were comparable, an exposure suitable for use with the probes was calculated from trial imaging experiments and was 100 to 200 ms (CM-H_2DCF-DA) or 400 to 500 ms (DAF-FM-DA). To allow comparisons between images, each experiment used identical exposures throughout, and at least one image was captured prior to treatment. Focus was checked and adjusted for drift if necessary. Quantification of relative fluorescence units was performed using the ImageJ software package. For experiments monitoring ROS and NO signals and for the cross talk experiments, the average pixel intensity for each pollen tube was measured in the shank region, using a 15- × 5-μm box 5 μm behind the tip, 20 μm in length; for the drug experiments, a 42 × 42 pixel box 15 μm from tip was used; for the SI experiments, a box corresponding to the first 100 μm of the pollen tube was used.

F-actin imaging and quantitation used a standard TX Red filter (Chroma Technology). Pollen tubes were scored as "normal" F-actin configuration, "actin foci," which is a typical marker induced by SI, and "intermediate" (not in either category). Twenty or 30 pollen tubes for each of three replicates were scored (a total of 70 pollen tubes scored for each treatment).

Pollen Protein Extraction and Caspase Activity Assays

Caspase extraction buffer (50 mM Na-acetate, 10 mM L-Cys, 10% [v/v] glycerol, and 0.1% [w/v] CHAPS), pH 6.0, was added to pollen. Samples were prepared, and the caspase-3-like/DEVDase activity present in pollen extracts was measured using the 7-amino-4-trifluoromethyl coumarin (AMC) substrate, Ac-DEVD-AMC (BioMol), as described (Bosch and Franklin-Tong, 2007). Release of fluorophore by cleavage was measured (excitation, 380 nm; emission, 460 nm) using a FLUOstar OPTIMA reader (BMG Labtech) at 27°C for 5 h. Duplicate samples were also incubated in parallel in the presence of 50 μM caspase 3/7-DEVDase inhibitor Ac-DEVD-CHO. All assays were performed on five independent samples, measured in duplicate. *P* values were calculated using a two-way ANOVA.

Supplemental Data

The following materials are available in the online version of this article.

Supplemental Figure S1. SI-induced ROS is inhibited by DPI.

Supplemental Figure S2. Verification of DEVDase activity in *Papaver* pollen.

Supplemental Figure S3. A proposed model for how ROS and NO might fit into the SI-PCD signaling network.

Supplemental Movie S1. Movie of SI-induced ROS increases measured using the CM-H_2DCF-DA probe.

Supplemental Movie S2. Movie of another typical SI-stimulated increase of ROS measured using the CM-H_2DCF-DA probe.

Supplemental Movie S3. Movie of an untreated pollen tube loaded with CM-H_2DCF-DA.

Supplemental Movie S4. Movie of an untreated pollen tube loaded with the DAF-FM-DA probe.

Supplemental Movie S5. Movie of SI-stimulated NO increases measured using the DAF-FM-DA probe.

Supplemental Movie S6. Movie of another typical SI-stimulated increase of NO measured using the DAF-FM-DA probe.

Received October 19, 2010; accepted March 4, 2011; published March 8, 2011.

LITERATURE CITED

Apel K, Hirt H (2004) Reactive oxygen species: metabolism, oxidative stress, and signal transduction. Annu Rev Plant Biol **55:** 373–399

Balcerczyk A, Soszynski M, Bartosz G (2005) On the specificity of 4-amino-5-methylamino-2′,7′-difluorofluorescein as a probe for nitric oxide. Free Radic Biol Med **39:** 327–335

Bánfi B, Tirone F, Durussel I, Knisz J, Moskwa P, Molnár GZ, Krause K-H, Cox JA (2004) Mechanism of Ca^{2+} activation of the NADPH oxidase 5 (NOX5). J Biol Chem **279:** 18583–18591

Besson-Bard A, Courtois C, Gauthier A, Dahan J, Dobrowolska G, Jeandroz S, Pugin A, Wendehenne D (2008) Nitric oxide in plants: production and cross-talk with Ca^{2+} signaling. Mol Plant **1:** 218–228

Bosch M, Franklin-Tong VE (2007) Temporal and spatial activation of caspase-like enzymes induced by self-incompatibility in *Papaver* pollen. Proc Natl Acad Sci USA **104:** 18327–18332

Bosch M, Poulter NS, Perry RM, Wilkins KA, Franklin-Tong VE (2010) Characterization of a legumain/vacuolar processing enzyme and YVADase activity in *Papaver* pollen. Plant Mol Biol **74:** 381–393

Cárdenas L, Martínez A, Sánchez F, Quinto C (2008) Fast, transient and specific intracellular ROS changes in living root hair cells responding to Nod factors (NFs). Plant J **56:** 802–813

Coelho SM, Brownlee C, Bothwell JH (2008) A tip-high, Ca^{2+}-interdependent, reactive oxygen species gradient is associated with polarized growth in *Fucus serratus* zygotes. Planta **227:** 1037–1046

Courtois C, Besson A, Dahan J, Bourque S, Dobrowolska G, Pugin A, Wendehenne D (2008) Nitric oxide signalling in plants: interplays with Ca^{2+} and protein kinases. J Exp Bot **59:** 155–163

Dalle-Donne I, Milzani A, Giustarini D, Di Simplicio P, Colombo R, Rossi R (2000) S-NO-actin: S-nitrosylation kinetics and the effect on isolated vascular smooth muscle. J Muscle Res Cell Motil **21:** 171–181

Dalle-Donne I, Rossi R, Milzani A, Di Simplicio P, Colombo R (2001) The actin cytoskeleton response to oxidants: from small heat shock protein

phosphorylation to changes in the redox state of actin itself. Free Radic Biol Med **31:** 1624–1632

de Graaf BHJ, Rudd JJ, Wheeler MJ, Perry RM, Bell EM, Osman K, Franklin FCH, Franklin-Tong VE (2006) Self-incompatibility in *Papaver* targets soluble inorganic pyrophosphatases in pollen. Nature **444:** 490–493

Delledonne M (2005) NO news is good news for plants. Curr Opin Plant Biol **8:** 390–396

Delledonne M, Zeier J, Marocco A, Lamb C (2001) Signal interactions between nitric oxide and reactive oxygen intermediates in the plant hypersensitive disease resistance response. Proc Natl Acad Sci USA **98:** 13454–13459

de Pinto MC, Tommasi F, De Gara L (2002) Changes in the antioxidant systems as part of the signaling pathway responsible for the programmed cell death activated by nitric oxide and reactive oxygen species in tobacco Bright-Yellow 2 cells. Plant Physiol **130:** 698–708

Foote HCC, Ride JP, Franklin-Tong VE, Walker EA, Lawrence MJ, Franklin FCH (1994) Cloning and expression of a distinctive class of self-incompatibility (S) gene from *Papaver rhoeas* L. Proc Natl Acad Sci USA **91:** 2265–2269

Foreman J, Demidchik V, Bothwell JH, Mylona P, Miedema H, Torres MA, Linstead P, Costa S, Brownlee C, Jones JD, et al (2003) Reactive oxygen species produced by NADPH oxidase regulate plant cell growth. Nature **422:** 442–446

Foyer CH, Noctor G (2005) Redox homeostasis and antioxidant signaling: a metabolic interface between stress perception and physiological responses. Plant Cell **17:** 1866–1875

Frahry G, Schopfer P (1998) Inhibition of O_2-reducing activity of horseradish peroxidase by diphenyleneiodonium. Phytochemistry **48:** 223–227

Franklin-Tong VE, editor (2008) Self-Incompatibility in Flowering Plants: Evolution, Diversity, and Mechanisms. Springer, Berlin

Franklin-Tong VE, Gourlay CW (2008) A role for actin in regulating apoptosis/programmed cell death: evidence spanning yeast, plants and animals. Biochemical J **413:** 389

Franklin-Tong VE, Hackett G, Hepler PK (1997) Ratio-imaging of $[Ca^{2+}]_i$ in the self-incompatibility response in pollen tubes of *Papaver rhoeas*. Plant J **12:** 1375–1386

Franklin-Tong VE, Holdaway-Clarke TL, Straatman KR, Kunkel JG, Hepler PK (2002) Involvement of extracellular calcium influx in the self-incompatibility response of *Papaver rhoeas*. Plant J **29:** 333–345

Franklin-Tong VE, Ride JP, Read ND, Trewavas AJ, Franklin FCH (1993) The self-incompatibility response in *Papaver rhoeas* is mediated by cytosolic-free calcium. Plant J **4:** 163–177

Frenkel SR, Clancy RM, Ricci JL, Di Cesare PE, Rediske JJ, Abramson SB (1996) Effects of nitric oxide on chondrocyte migration, adhesion, and cytoskeletal assembly. Arthritis Rheum **39:** 1905–1912

Gechev TS, Van Breusegem F, Stone JM, Denev I, Laloi C (2006) Reactive oxygen species as signals that modulate plant stress responses and programmed cell death. Bioessays **28:** 1091–1101

Geitmann A, Snowman BN, Emons AMC, Franklin-Tong VE (2000) Alterations in the actin cytoskeleton of pollen tubes are induced by the self-incompatibility reaction in *Papaver rhoeas*. Plant Cell **12:** 1239–1251

Halliwell B, Whiteman M (2004) Measuring reactive species and oxidative damage in vivo and in cell culture: how should you do it and what do the results mean? Br J Pharmacol **142:** 231–255

Hempel SL, Buettner GR, O'Malley YQ, Wessels DA, Flaherty DM (1999) Dihydrofluorescein diacetate is superior for detecting intracellular oxidants: comparison with 2′,7′-dichlorodihydrofluorescein diacetate, 5(and 6)-carboxy-2′,7′-dichlorodihydrofluorescein diacetate, and dihydrorhodamine 123. Free Radic Biol Med **27:** 146–159

Kakeda K, Jordan ND, Conner A, Ride JP, Franklin-Tong VE, Franklin FCH (1998) Identification of residues in a hydrophilic loop of the *Papaver rhoeas* S protein that play a crucial role in recognition of incompatible pollen. Plant Cell **10:** 1723–1732

Kasprowicz A, Szuba A, Volkmann D, Baluska F, Wojtaszek P (2009) Nitric oxide modulates dynamic actin cytoskeleton and vesicle trafficking in a cell type-specific manner in root apices. J Exp Bot **60:** 1605–1617

Kim S-J, Hwang S-G, Kim I-C, Chun J-S (2003) Actin cytoskeletal architecture regulates nitric oxide-induced apoptosis, dedifferentiation, and cyclooxygenase-2 expression in articular chondrocytes via mitogen-activated protein kinase and protein kinase C pathways. J Biol Chem **278:** 42448–42456

Knight H, Trewavas AJ, Knight MR (1996) Cold calcium signaling in *Arabidopsis* involves two cellular pools and a change in calcium signature after acclimation. Plant Cell **8:** 489–503

Kwak JM, Mori IC, Pei ZM, Leonhardt N, Torres MA, Dangl JL, Bloom RE, Bodde S, Jones JD, Schroeder JI (2003) NADPH oxidase *AtrbohD* and *AtrbohF* genes function in ROS-dependent ABA signaling in Arabidopsis. EMBO J **22:** 2623–2633

Kwak JM, Nguyen V, Schroeder JI (2006) The role of reactive oxygen species in hormonal responses. Plant Physiol **141:** 323–329

Laloi C, Apel K, Danon A (2004) Reactive oxygen signalling: the latest news. Curr Opin Plant Biol **7:** 323–328

Li S, Samaj J, Franklin-Tong VE (2007) A mitogen-activated protein kinase signals to programmed cell death induced by self-incompatibility in *Papaver* pollen. Plant Physiol **145:** 236–245

Li Y, Trush MA (1998) Diphenyleneiodonium, an NAD(P)H oxidase inhibitor, also potently inhibits mitochondrial reactive oxygen species production. Biochem Biophys Res Commun **253:** 295–299

Lindermayr C, Saalbach G, Durner J (2005) Proteomic identification of *S*-nitrosylated proteins in Arabidopsis. Plant Physiol **137:** 921–930

McInnis SM, Desikan R, Hancock JT, Hiscock SJ (2006) Production of reactive oxygen species and reactive nitrogen species by angiosperm stigmas and pollen: potential signalling crosstalk? New Phytol **172:** 221–228

Mittler R, Vanderauwer S, Gollery M, van Breusegem F (2004) Reactive oxygen gene network of plants. Trends Plant Sci **9:** 490–498

Moldovan L, Moldovan NI, Sohn RH, Parikh SA, Goldschmidt-Clermont PJ (2000) Redox changes of cultured endothelial cells and actin dynamics. Circ Res **86:** 549–557

Monshausen GB, Bibikova TN, Messerli MA, Shi C, Gilroy S (2007) Oscillations in extracellular pH and reactive oxygen species modulate tip growth of Arabidopsis root hairs. Proc Natl Acad Sci USA **104:** 20996–21001

Moreau M, Lindermayr C, Durner J, Klessig DF (2010) NO synthesis and signaling in plants: where do we stand? Physiol Plant **138:** 372–383

Neill S, Barros R, Bright J, Desikan R, Hancock J, Harrison J, Morris P, Ribeiro D, Wilson I (2008) Nitric oxide, stomatal closure, and abiotic stress. J Exp Bot **59:** 165–176

Neill S, Desikan R, Hancock J (2002) Hydrogen peroxide signalling. Curr Opin Plant Biol **5:** 388–395

Planchet E, Kaiser WM (2006) Nitric oxide (NO) detection by DAF fluorescence and chemiluminescence: a comparison using abiotic and biotic NO sources. J Exp Bot **57:** 3043–3055

Potocký M, Jones MA, Bezvoda R, Smirnoff N, Zárský V (2007) Reactive oxygen species produced by NADPH oxidase are involved in pollen tube growth. New Phytol **174:** 742–751

Poulter NS, Bosch M, Franklin-Tong VE (February 13, 2011) Proteins implicated in mediating self-incompatibility-induced alterations to the actin cytoskeleton of *Papaver* pollen. Ann Bot (Lond) http://dx.doi.org/10.1093/aob/mcr022

Poulter NS, Staiger CJ, Rappoport JZ, Franklin-Tong VE (2010) Actin-binding proteins implicated in the formation of the punctate actin foci stimulated by the self-incompatibility response in *Papaver*. Plant Physiol **152:** 1274–1283

Poulter NS, Vatovec S, Franklin-Tong VE (2008) Microtubules are a target for self-incompatibility signaling in *Papaver* pollen. Plant Physiol **146:** 1358–1367

Prado AM, Porterfield DM, Feijó JA (2004) Nitric oxide is involved in growth regulation and re-orientation of pollen tubes. Development **131:** 2707–2714

Riganti C, Gazzano E, Polimeni M, Costamagna C, Bosia A, Ghigo D (2004) Diphenyleneiodonium inhibits the cell redox metabolism and induces oxidative stress. J Biol Chem **279:** 47726–47731

Rudd JJ, Franklin-Tong VE (1999) Calcium signaling in plants. Cell Mol Life Sci **55:** 214–232

Rudd JJ, Osman K, Franklin FCH, Franklin-Tong VE (2003) Activation of a putative MAP kinase in pollen is stimulated by the self-incompatibility (SI) response. FEBS Lett **547:** 223–227

Sagi M, Fluhr R (2001) Superoxide production by plant homologues of the $gp91^{phox}$ NADPH oxidase: modulation of activity by calcium and by tobacco mosaic virus infection. Plant Physiol **126:** 1281–1290

Shin R, Schachtman DP (2004) Hydrogen peroxide mediates plant root cell

response to nutrient deprivation. Proc Natl Acad Sci USA **101:** 8827–8832

Snowman BN, Kovar DR, Shevchenko G, Franklin-Tong VE, Staiger CJ (2002) Signal-mediated depolymerization of actin in pollen during the self-incompatibility response. Plant Cell **14:** 2613–2626

Takayama S, Isogai A (2005) Self-incompatibility in plants. Annu Rev Plant Biol **56:** 467–489

Thomas SG, Franklin-Tong VE (2004) Self-incompatibility triggers programmed cell death in *Papaver* pollen. Nature **429:** 305–309

Thomas SG, Huang S, Li S, Staiger CJ, Franklin-Tong VE (2006) Actin depolymerization is sufficient to induce programmed cell death in self-incompatible pollen. J Cell Biol **174:** 221–229

Torres MA, Dangl JL, Jones JDG (2002) Arabidopsis gp91^{phox} homologues *AtrbohD* and *AtrbohF* are required for accumulation of reactive oxygen intermediates in the plant defense response. Proc Natl Acad Sci USA **99:** 517–522

Torres MA, Onouchi H, Hamada S, Machida C, Hammond-Kosack KE, Jones JDG (1998) Six *Arabidopsis thaliana* homologues of the human respiratory burst oxidase (*gp91^{phox}*). Plant J **14:** 365–370

Van Breusegem F, Bailey-Serres J, Mittler R (2008) Unraveling the tapestry of networks involving reactive oxygen species in plants. Plant Physiol **147:** 978–984

Van Breusegem F, Dat JF (2006) Reactive oxygen species in plant cell death. Plant Physiol **141:** 384–390

Wang C-L, Wu J, Xu G-H, Gao YB, Chen G, Wu J-Y, Wu HQ, Zhang S-L (2010) S-RNase disrupts tip-localized reactive oxygen species and induces nuclear DNA degradation in incompatible pollen tubes of *Pyrus pyrifolia*. J Cell Sci **123:** 4301–4309

Wang Y, Yun B-W, Kwon E, Hong JK, Yoon J, Loake GJ (2006) S-Nitrosylation: an emerging redox-based post-translational modification in plants. J Exp Bot **57:** 1777–1784

Wardman P (2007) Fluorescent and luminescent probes for measurement of oxidative and nitrosative species in cells and tissues: progress, pitfalls, and prospects. Free Radic Biol Med **43:** 995–1022

Wendehenne D, Durner J, Klessig DF (2004) Nitric oxide: a new player in plant signalling and defence responses. Curr Opin Plant Biol **7:** 449–455

Wheeler MJ, de Graaf BHJ, Hadjiosif N, Perry RM, Poulter NS, Osman K, Vatovec S, Harper A, Franklin FCH, Franklin-Tong VE (2009) Identification of the pollen self-incompatibility determinant in *Papaver rhoeas*. Nature **459:** 992–995

Wu J, Wang S, Gu Y, Zhang S, Publicover SJ, Franklin-Tong VE (2011) Self-incompatibility in *Papaver rhoeas* activates nonspecific cation conductance permeable to Ca^{2+} and K^+. Plant Physiol **155:** 963–973

Yao N, Greenberg JT (2006) *Arabidopsis* ACCELERATED CELL DEATH2 modulates programmed cell death. Plant Cell **18:** 397–411

Zago E, Morsa S, Dat JF, Alard P, Ferrarini A, Inzé D, Delledonne M, Van Breusegem F (2006) Nitric oxide- and hydrogen peroxide-responsive gene regulation during cell death induction in tobacco. Plant Physiol **141:** 404–411

Zaninotto F, La Camera S, Polverari A, Delledonne M (2006) Cross talk between reactive nitrogen and oxygen species during the hypersensitive disease resistance response. Plant Physiol **141:** 379–383